

1 **WAVELET ANALYSIS OF THE SINGULAR SPECTRAL RECONSTRUCTED TIME SERIES TO STUDY**  
2 **THE IMPRINTS OF SOLAR-ENSO-GEOMAGNETIC ACTIVITY ON INDIAN CLIMATE**

3  
4 **<sup>1</sup>S. Sri Lakshmi\* and <sup>2</sup>R. K. Tiwari**

5  
6 <sup>1</sup> University Centre for Earth and Space Sciences, University of Hyderabad, Hyderabad 500 046,  
7 India

8 <sup>2</sup> CSIR-National Geophysical Research Institute, Uppal Road, Hyderabad 500 007, India

9  
10 **\*Corresponding Author:** srilakshmi.ucess@gmail.com  
11 Tel.: +91-40-23132671 (Office)  
12 Fax: +91-40-23010152  
13

14 **ABSTRACT**

15 To study the imprints of the Solar-ENSO-Geomagnetic activity on the Indian Subcontinent, we  
16 have applied the Singular spectral analysis (SSA) and wavelet analysis to the tree ring  
17 temperature variability record from the Western Himalayas. Other data used in the present  
18 study are the Solar Sunspot Number (SSN), Geomagnetic Indices (aa Index) and Southern  
19 Oscillation Index (SOI) for the common time period of 1876-2000. Both SSA and wavelet  
20 spectral analyses reveal the presence of 5-7 years short term ENSO variations and the 11 year  
21 solar cycle indicating the possible combined influences of solar-geomagnetic activities and  
22 ENSO on the Indian temperature. Another prominent signal corresponding to 33-year  
23 periodicity in the tree ring record suggests the Sun-temperature variability link probably  
24 induced by changes in the basic state of the earth's atmosphere. In order to complement the  
25 above findings, we performed a wavelet analysis of SSA reconstructed time series, which agrees  
26 well with our earlier results and ~~also~~ increases the signal to noise ratio thereby showing strong  
27 influence of solar-geomagnetic activity & ENSO throughout the entire ~~time~~ period. The solar  
28 flares are considered ~~to be~~ responsible for causing the atmospheric circulation patterns. The  
29 net effect of solar-geomagnetic processes on the temperature record might suggest  
30 counteracting influences on shorter (about 5–6 y) and longer (about 11–12 y) time scales. The  
31 present analyses suggest that the influence of solar activities on the Indian temperature  
32 variability operates in part indirectly through coupling of ENSO on multilateral time scales. The

33 analyses, hence, provide credible evidence for tele-connections of tropical pacific climatic  
34 variability and Indian climate ranging from inter-annual-decadal time scales and also suggest  
35 the possible role of exogenic triggering in reorganizing the global earth-ocean-atmospheric  
36 systems.

37 **Key words:** *Geomagnetic activity, Western Himalayas, Sunspot Number, SOI index, Singular*  
38 *spectral analysis, Wavelet spectrum, Coherency.*

39

#### 40 **1. Introduction:**

41 Several recent studies of solar/geomagnetic effects on climate have been examined on both  
42 global as well as on regional scales (Lean and Rind, 2008; Benestaed and Schmidt, 2009; Meehl,  
43 2009; Kiladis and Diaz 1989; Pant and Rupa Kumar 1997; Gray et al. 1992; Wiles et al. 1998; Friis  
44 and Svensmark 1997; Rigozo et al. 2005; Feng et al. 2003; Tiwari and srilakshmi 2009; Chowdary  
45 et al. 2006, 2014; Appenzeller et al. 1998; Proctor et al. 2002; Tsonis et al. 2005; Freitas and  
46 Mclean 2013). The Sun's long-term magnetic variability caused by the sunspots is considered as  
47 one of the primary drivers of climatic changes. The short-term magnetic variability is due to the  
48 disturbances in Earth's magnetic fields caused by the solar activities and is indicated by the  
49 geomagnetic indices. The Sun's magnetic variability modulates the magnetic and particulate  
50 fluxes in the heliosphere. This determines the interplanetary conditions and imposes significant  
51 electromagnetic forces and effects upon the planetary atmosphere. All these effects are due to  
52 the changing solar-magnetic fields, which are relevant for planetary climates including the  
53 climate of the Earth. The Sun-Earth relationship varies on different time scales ranging from  
54 days to years bringing a drastic influence on the climatic patterns. The ultimate cause of solar  
55 variability, at time scales from decadal to centennial to millennial or even longer scales has its  
56 origin in the solar dynamo mechanism. During the solar maxima, huge amounts of solar energy  
57 particles are released, thereby causing the geomagnetic disturbances. The 11 years solar cycle  
58 acts as an important driving force for variations in the space weather, ultimately giving rise to  
59 climatic changes. It is, therefore, imperative to understand the origin of space climate by  
60 analyzing the different proxies of solar magnetic variabilities. Another important phenomenon  
61 is El Nino-Southern Oscillation (ENSO), which associated with droughts, floods and intense

62 rainfall in different parts of the world. The strong coupling and interactions between the  
63 Tropical Ocean and the atmosphere play a major role in the development of the global climatic  
64 system. The El Nino events generally recur approximately every 3-5 years with large events  
65 spaced around 3-7 years apart. The ENSO phenomena have shown huge impact on the Asian  
66 monsoon (Cole et. al., 1993), Indian monsoon (Chowdary et al. 2006, 2014) as well as globally  
67 (Horel and Wallance 1981; Barnett 1989; Yasunari 1985; Nicholson 1997). In particular, the El  
68 Nino, solar, geomagnetic activities are the major affecting forces on the decadal and  
69 interdecadal temperature variability on global and regional scales in a direct/indirect way (El-  
70 Borie et al, 2010; Gray et al., 2010). Recent studies (Frohlich and Lean 2004; Steinhilber et al.  
71 2009) indicate the possible influence of solar activity on Earth's temperature/climate on multi-  
72 decadal time scales. The 11 year solar cyclic variations observed from the several temperature  
73 climate records also suggest the impact of solar irradiance variability on terrestrial temperature  
74 (Budyko 1969; Friis and Lassen 1991; Friis and Svensmark 1997; Kasatkina et al. 2007). The bi-  
75 decadal (22 years) called the Hale cycle, is related to the reversal of the solar magnetic field  
76 direction (Lean et al. 1995; Kasatkina et al. 2007). The 33 year cycle (Bruckener cycle) is also  
77 caused by the solar origin, but it is a very rare cycle (Kasatkina et al. 2007). The 2-7 years ENSO  
78 cyclic pattern and its possible coupling process is the major driving force for the temperature  
79 variability (Gray et al. 1992; Wiles et al. 1998; Mokhov et al. 2000; Rigozo et al. 2007, Kothawale  
80 et al. 2010). El-Borie and Al-Thoyaib, 2006; El-Borie et al., 2007 and El-Borie et al, 2010 have  
81 indicated in their studies that the global temperature should lag the geomagnetic activity with a  
82 maximum correlation when the temperature lags by 6 years. Mendoza et. al., 1991 reported on  
83 possible connections between solar activity and El Nino's, while Reid and Gage (1988) and Reid  
84 (1991) reported on the similarities between the 11-year running means of monthly sunspot  
85 numbers and global sea surface temperature. These findings suggest that there is a possibility  
86 of strong coupling between temperature-ENSO and solar-geomagnetic signals.

87 ~~The mean global temperature of the Earth's surface also plays a very important role in~~  
88 ~~bringing climatic changes.~~ Several studies have been carried out to understand the ~~detailed~~  
89 climatic changes of India in the past millennium using various proxy records e.g. ice cores, lake  
90 sediments, glacier fluctuations, peat deposits etc. There is a lack of high-precision and high-

91 resolution palaeo-climatic information for longer time scale from the Indian subcontinent. Tree-  
92 ring data is a promising proxy to retrieve high resolution past climatic changes from several  
93 geographical regions of India (Bhattacharyya et al. 1988; Bhattacharyya et al. 1992; Hughes,  
94 1992; Bhattacharyya and Yadav, 1996; Borgaonkar et al. 1996; Chaudhary et al. 1999; Yadav et  
95 al. 1999; Bhattacharyya and Chaudhary, 2003; Bhattacharyya et al. 2006; Shah et al. 2007) It  
96 has been noted that tree-ring based climatic reconstructions in India generally do not exceed  
97 beyond 400 years records except at some sites in the Northwest Himalaya. Thus, a long record  
98 of tree-ring data is needed to extend available climate reconstruction further back to determine  
99 climatic variability on sub-decadal, decadal and century scale. However, non-availability of  
100 older living trees in most of the sites is hindering the preparation of long tree chronology. In a  
101 previous study (Tiwari and Srilakshmi, 2009), we have studied the periodicities and non-  
102 stationary modes in the tree ring temperature data from the same region (AD 1200-2000). To  
103 reveal significant connections among the Solar-geomagnetic-ENSO 'triad' phenomena on tree  
104 ring width in detail for the period from 1876-2000, we have applied here the Singular spectral  
105 analysis (SSA) and the wavelet spectral analysis for Sunspot data, geomagnetic data (aa index),  
106 Troup Southern Oscillation Index (SOI) and the Western Himalayas tree ring data. Here our  
107 main objective is to employ wavelet-based analysis on SSA reconstructed time series to find out  
108 the evidence of the possible linkages, if any, among ENSO-solar-geomagnetic in the Indian  
109 temperature records.

110

## 111 **2. Source and Nature of Data:**

112 The data analyzed here includes the time series of (1) Smoothed Sunspot number for solar  
113 activity (2) Geomagnetic activity data (aa indices) (3) Troup Southern Oscillation Index (SOI) for  
114 the study of El Nino-Southern Oscillation called ENSO (4) Western Himalayan temperature  
115 variability record. All the data sets have been analyzed for the common period of 125 years  
116 spanning over 1876-2000. The monthly sunspot number data has been obtained from the  
117 Sunspot Index Data Center [http:// astro.oma.be/SIDC/](http://astro.oma.be/SIDC/). The Troup SOI data is obtained from the  
118 Bureau of Meteorology of Australia, <http://www.bom.gov.au/climate/>. The data for  
119 geomagnetic activity, aa Index, was provided by the National Geophysical Data Center, NGDC,

120 (<http://www.ngdc.noaa.gov/stp/GEOMAG/aastar.shtml>). The aa index is a measure of  
121 disturbances level of Earth's magnetic field based on magnetometer observations at two, nearly  
122 antipodal, stations in Australia and England. In recent studies, the tree ring proxy climate  
123 indicators are being used for extracting information regarding past seasonal temperature or  
124 precipitation/drought based on the measurements of annual ring width. The detailed  
125 description of the data has been presented elsewhere (Yadav et. al., 2004). A brief account of  
126 the data pertinent to the present analysis, however, is summarized here. The tree ring data  
127 being analyzed here is one of the best temperature variability records (1876 to 2000) of the  
128 pre-monsoon season in the Western Himalayas available. The mean temperature series is  
129 obtained from nine weather stations including both from high and low elevation areas in the  
130 Western Himalayas. Temperature variability history is based on widely spread pure Himalayan  
131 cedar (*Cedrus deodara* (Roxb.) G. Don) trees and characterizes all the sites with almost no  
132 ground vegetation and thereby minimizes individual variation in tree-ring sequences induced by  
133 inter tree competition (Yadav et. al., 2004). The mean chronological structure is based on in  
134 total 60 radii from 45 trees in total, statistical feature of which show that the chronology is  
135 suitable for dendro-climatic studies back to AD 1226 (Yadav et. al., 2004).

136

137 **3. Methods applied:** To analyze the temporal series and to find the climatic structure, we have  
138 here three methods: Principal component analysis (PCA), Singular Spectral analysis (SSA) and  
139 wavelet analysis.

140 **3.1. Principal component analysis (PCA):** As a preliminary analysis, we have applied the  
141 Principal component analysis (PCA) to the data sets for the reduction and extraction of  
142 dimensionality of the data and to rate the amount of variation present in the original data set.  
143 The purpose to apply the PCA is to identify patterns in the given time series. The new  
144 components thereby obtained by the PCA analysis are termed as PC1, PC2, PC3 and so on, (for  
145 the first, second and third principal components), and are uncorrelated. The different PCs  
146 capture part of the variance and are ranked depending on their corresponding percentage  
147 variance.

148

149 **3.2. Singular spectral analysis:** The Singular Spectrum Analysis (SSA) method is designed to  
 150 extract as much information as possible from a short, noisy time series without any prior  
 151 knowledge about the dynamics underlying the series (Broomhead and King, 1986; Vautard and  
 152 Ghil, 1989; Alonso et. al., 2005; Golyandina et al., 2001). The method is a form of principal  
 153 component analysis (PCA) applied to lag-correlations structures of the time series. The basic  
 154 SSA decomposes an original time series into a new series which consists of trend, periodic or  
 155 quasi-periodic and white noises according to the singular value decomposition (SVD) and  
 156 provides the reconstructed components (RCs). The basic steps involved in SSA are:  
 157 decomposition (involves embedding, singular value decomposition (SVD)) and reconstruction  
 158 (involves grouping and diagonal averaging). Embedding decomposes the original time series  
 159 into the trajectory matrix; SVD turns the trajectory matrix into the decomposed trajectory  
 160 matrices. The reconstruction stage involves grouping to make subgroups of the decomposed  
 161 trajectory matrices and diagonal averaging to reconstruct the new time series from the  
 162 subgroups.

163 **Step1: Decomposition:**

164 **(a) Embedding:** The first step in the basic SSA algorithm is the embedding step where  
 165 the initial time series change into the trajectory matrix. Let the time series be  $Y = \{y_1, \dots, y_N\}$   
 166 of length  $N$  without any missing values. Here the window length  $L$  is chosen such that  $2 < L <$   
 167  $N/2$  to embed the initial time series. We map the time series  $Y$  into the  $L$  lagged vectors,  $Y_i =$   
 168  $\{y_i, \dots, y_{i+L-1}\}$  for  $i = 1, \dots, K$ , where  $K = N - L + 1$ . The trajectory matrix  $T_Y$  ( $L \times K$  dimensions) is

169 written as:  $T_Y = \begin{pmatrix} Y_1 \\ Y_2 \\ \cdot \\ \cdot \\ Y_K \end{pmatrix} \dots\dots\dots(1)$

170 **(b) Singular Value Decomposition (SVD):** Here we apply SVD to the trajectory matrix  $T_Y$   
 171 to decompose and obtain  $T_Y = UDV'$  called eigentriples; where  $U_i$  ( $K \times L$  dimensions;  $1 < i < L$ ) is an  
 172 orthonormal matrix;  $D_i$  ( $1 < i < L$ ) is a diagonal matrix of order  $L$ ;  $V_i$  ( $L \times L$  dimensions;  $1 < i < L$ ) is  
 173 a square orthonormal matrix.

174 The trajectory matrix is thus written as  $T_Y = \sum_{i=1}^d U_i \sqrt{\lambda_i} V_i^T$ ; .....(2)

175 where the  $i^{\text{th}}$  Eigen triple of  $T_i = U_i \times \sqrt{\lambda_i} \times V_i^T$ ,  $i = 1, 2, 3, \dots, d$  in which  $d = \max(i: \sqrt{\lambda_i} > 0)$ .

176 **Step 2: Reconstruction:**

177 **(c) Grouping:** Here the matrix  $T_i$  is decomposed into subgroups according to the trend,  
 178 periodic or quasi-periodic components and white noises. The grouping step of the  
 179 reconstruction stage corresponds to the splitting of the elementary matrices  $T_i$  into several  
 180 groups and summing the matrices within each group. Let  $I = \{i_1, i_2, \dots, i_p\}$  be the group of indices  
 181  $i_1, \dots, i_p$ . Then the matrix  $T_I$  corresponding to the group  $I$  is defined as  $T_I = T_{i_1} + T_{i_2} + \dots + T_{i_p}$ . The split of  
 182 the set of indices  $J = 1, 2, \dots, d$  into the disjoint subsets  $I_1, I_2, \dots, I_m$  corresponds to the equation  
 183 (3):

184 
$$T = T_{I_1} + T_{I_2} + \dots + T_{I_m}. \quad \dots\dots\dots(3)$$

185 The sets  $I_1, \dots, I_m$  are called the eigen triple grouping.

186 **(d) Diagonal averaging:** The diagonal averaging transfers each matrix  $T$  into a time  
 187 series, which is an additive component of the initial time series  $Y$ . If  $z_{ij}$  stands for a element  
 188 matrix  $Z$ , the  $k$ th term of the resulting series is obtained by averaging  $z_{ij}$  over all  $i, j$  such that  
 189  $i+j=k+2$ . This is called diagonal averaging or the Hankelization of the matrix  $Z$ . The Hankel matrix  
 190  $HZ$ , is the trajectory matrix corresponding to the series obtained by the result of diagonal  
 191 averaging.

192 Considering equation (3), let  $X$  ( $L \times K$ ) matrix with elements  $x_{ij}$ , where  $1 \leq i \leq L$ ,  $1 \leq j \leq K$ .  
 193 Here diagonal averaging transforms matrix  $X$  to a series  $g_0, \dots, g_{T-1}$  using the formula:

194 
$$g_k = \begin{cases} \frac{1}{k+1} \sum_{m=1}^{k+1} x_{m, k-m+2}^* & 0 \leq k < L^* - 1 \\ \frac{1}{L^*} \sum_{m=1}^{L^*} x_{m, k-m+2}^* & L^* - 1 \leq k < K^* \\ \frac{1}{T-k} \sum_{m=k-k^*+2}^{N-k+1} x_{m, k-m+2}^* & K^* - 1 \leq k < T \end{cases} \quad (4)$$

195 This diagonal averaging by equation (4) applied to the resultant matrix  $X_{In}$ , produces time series  
 196  $Y_n$  of length  $T$ . For such signal characteristics, it is essential to examine the time-frequency

197 pattern as to understand whether a particular frequency is temporally consistent or  
198 inconsistent. Hence for non-stationary signals, we need a transform that will be useful to obtain  
199 the frequency content of the time series/signal as a function of time.

200 An alternative method for studying the non-stationarity of the time series is wavelet  
201 transform. For non-stationary signals, wavelets decomposition would be the most appropriate  
202 method because the analyzing functions (the wavelets function) are localized both in time and  
203 frequency.

204  
205 **3.3. Wavelet spectral analysis:** During the past decades, wavelet analysis has become a popular  
206 method for the analysis of aperiodic and quasi-periodic data (Grinsted et. al., 2004; Jevrejeva  
207 et. al., 2003; Torrence and Compo, 1998; Torrence and Webster, 1999). In particular, it has  
208 become an important tool for studying localized variations of power within a time series. By  
209 decomposing a time series into time-frequency space, the dominant modes of variability and  
210 their variation with respect to time can be identified. The wavelet transform has various  
211 applications in geophysics, including tropical convection (Weng and Lau 1994), the El Niño–  
212 Southern Oscillation (Gu and Philander 1995), etc. We have applied the wavelet analysis to  
213 analyze the non-stationary signals which permits the identification of main periodicities of  
214 ENSO-sunspot-geomagnetic in the time series. The results give us more insight information  
215 about the evolution of these variables in frequency-time mode.

216 A wavelet transform requires the choice of analyzing function  $\Psi$  (called “mother  
217 wavelet”) that has the specific property of time-frequency localization. The continuous wavelet  
218 transform revolves around decomposing the time series into scaling components for identifying  
219 oscillations occurring at fast (time) scale and other at slow scales. Mathematically, the  
220 continuous wavelets transform of a time series  $f(t)$  can be given as:

221 
$$W_{\psi}(f)(a, b) = \frac{1}{\sqrt{a}} \int_{-\infty}^{\infty} f(t) \psi\left(\frac{t-b}{a}\right) dt \dots\dots\dots(5)$$

222 Here  $f(t)$  represents time series,  $\Psi$  is the base wavelets function (here we have chosen the  
223 Morlet function), with length that is much shorter than the time series  $f(t)$ .  $W$  stands for



224 wavelet coefficients. The variable 'a' is called the scaling parameter that determines the  
225 frequency (or scale) so that varying 'a' gives rise to wavelet spectrum. The factor 'b' is related to  
226 the shift of the analysis window in time so that varying b represents the sliding method of the  
227 wavelet over f(t).

228 In several recent analyses, complex Morlet wavelet has been found useful for  
229 geophysical time series analysis. The Morlet is mostly used to find out areas where there is high  
230 amplitude at certain frequencies. The complex Morlet wavelet can be represented by a periodic  
231 sinusoidal function with a Gaussian envelope and is excellent for Morlet wavelet may be  
232 defined mathematically, as follows:

233 
$$\psi(t) = \pi^{-1/4} e^{-i\omega_0 t} e^{-t^2/2} \dots\dots\dots(6)$$

234 where  $\omega_0$  is a non-dimensional value.  $\omega_0$  is chosen to be 5 to make the highest and lowest  
235 values of  $\psi$  approximately equal to 0.5, thus making the admissibility condition satisfied. The  
236 complex valued Morlet transform enables to extract information about the amplitude and  
237 phase of the signal to be analyzed. Wavelet transform preserves the self-similarity scaling  
238 property, which is the inherent characteristic feature of deterministic chaos. The continuous  
239 wavelet transform has edge artifacts because the wavelet is completely localized in time. The  
240 cone of influence (COI) is the area in which the wavelet power caused by a discontinuity at the  
241 edge has dropped to  $e^{-2}$  of the value to the edge. The statistical significance of the wavelet  
242 power can be assessed relative to the null hypotheses that the signal is generated by a  
243 stationary process with a given background power spectrum ( $P_k$ ) of first order autoregressive  
244 (AR1) process. (Grinsted et. al., 2004)

245 
$$P_k = \frac{1 - \alpha^2}{|1 - \alpha e^{-2i\pi k}|^2} \dots\dots\dots(7)$$

246 where k is Fourier frequency index.

247 The cross wavelet transform is applied to two time series to identify the similar patterns  
248 which are difficult to assess from a continuous wavelet map. Cross wavelet power reveals areas

249 with high common power. The cross wavelet of two time series  $x(t)$  and  $y(t)$  is defined as  $W^{XY} =$   
 250  $W^X W^{Y*}$ , where  $*$  denotes complex conjugate. The cross wavelet power of two time series with  
 251 background power spectra  $P_k^X$  and  $P_k^Y$  is given as

$$252 \quad D \left( \frac{|W_n^X(s)W_n^{Y*}(s)|}{\sigma_X \sigma_Y} < p \right) = \frac{Z_v(p)}{v} \sqrt{P_k^X P_k^Y}, \dots\dots\dots(8)$$

253 where  $Z_v(p)$  is the confidence level associated with the probability  $p$  for a pdf defined by the  
 254 square root of the product of the two  $\chi^2$  distributions (Torrence and Compo, 1998). The  
 255 wavelet power is  $|W_n^X(s)|^2$  and the complex argument of  $|W_n^X(s)|$  can be interpreted as the local  
 256 phase. The cross wavelet analysis gives the correlation between the two time series as function  
 257 of period of the signal and its time evolution with a 95% confidence level contour. The  
 258 statistical significance is estimated using red noise model.

259 Wavelet coherence is another important measure to assess how coherent the cross  
 260 wavelet spectrum transform is in time frequency space. The wavelet coherence of two time  
 261 series is defined as (Torrence and Webster, 1998)

$$262 \quad R_n^2(s) = \frac{|S(s^{-1} W_n^{XY}(s))|^2}{S(s^{-1} |W_n^X(s)|^2) \cdot S(s^{-1} |W_n^Y(s)|^2)} \dots\dots\dots(9)$$

263 where  $S$  is a smoothing operator. The smoothing operator is written as  $S(W) = S_{scale}(S_{time}$   
 264  $(W_n(s)))$ , where  $S_{scale}$  denotes smoothing along the wavelet scale axis and  $S_{time}$  smoothing in  
 265 time. Here for the morelet wavelet, the smoothing operator is

$$266 \quad S_{time}(W)|_s = \left( W_n(s) * c_1 \frac{-t^2}{2s^2} \right) \dots\dots\dots(10)$$

$$267 \quad S_{time}(W)|_s = (W_n(s) * c_2 \Pi(0.6s))_n \dots\dots\dots(11)$$

268 Where  $c_1$  and  $c_2$  are normalization constants and  $n$  is the rectangle function. The factor of 0.6 is  
 269 empirically determined scale decorrelation length of the Morlet wavelet (Torrence and Compo,

270 1998). The statistical significance level of the wavelet coherence is estimated using the Monte  
271 Carlo methods (Grinsted et. al., 2004).

272

#### 273 **4. Results and Discussion:**

274 We analyzed the data sets spanning over the period of 1876-2000 using the PCA, SSA and  
275 wavelet spectral analyses. Figure 1 shows four time series: (1) Smoothed Sunspot number  
276 representing solar activities; (2) Geomagnetic (aa indices); (3) Troup Southern Oscillation Index  
277 (SOI) for the study of ENSO and (4) Western Himalayan temperature variability record that are  
278 analyzed in the present work. From visual inspection it is apparent from Fig. 1 that both WH  
279 and SOI data show irregular and random pattern, while sunspot numbers have quasi- cyclic  
280 character. Further WH tree ring record also exhibits distinct temperature variability but  
281 nonstationary behavior at different scales. This variability might be suggestive of coupled global  
282 ocean-atmospheric dynamics or some other factors, such as deforestation, anthropogenic, high  
283 latitudinal influence etc (Yadav et. al., 2004).

284

#### (Figure 1)

285 Hence it is quite difficult to differentiate such a complex climate signals visually and difficult to  
286 infer any clear oscillation without the help of powerful mathematical methods. For  
287 identification of any oscillatory components and understanding the climatic variations on  
288 regional and global scale, we have applied the PCA, SSA and wavelet analysis. Figure 2 shows  
289 the principal components (PCs) for the first four eigen triples (PC1, PC2, PC3, PC4) for the given  
290 data sets. Figure 3 shows the power spectra of the principal components (PCs) for the four data  
291 sets shown in figure 2. From the figure 3, it is observed that the power spectra of PC1-4 for the  
292 sunspot data exhibits high power at 124, 11, 4-2.8 years. The presence of high solar signal at  
293 124 years indicates the quasi-stable oscillatory components in the data. The power spectra of  
294 geomagnetic data also shows the presence of strong signals at 124, 10-11, 4-2 years suggesting  
295 a strong link of solar-geomagnetic activity. The power spectra of WH temperature data shows  
296 strong high power at -62 years, 32-35 years, 11 years, 5 years and 2-3 years suggesting a  
297 strong combined influence of global ocean-atmospheric circulation, solar-geomagnetic and -  
298 ENSO effects on the Indian climate system. Climate cycles of 50-70 years have been widely

299 [reported in various ocean and atmospheric phenomena \(Ogurtsov, et al. 2002, Tiwari, 2005\).](#)  
300 [Schiesinger and Ramankutt \(1994\), Minobe \(1997\) have reported similar 55-70 year inter](#)  
301 [decadal oscillations in global mean temperature.](#) Dominant amplitudes ~~is found at 32-35 years~~  
302 corresponding to [62 and 32-35 years periodicities may, therefore, be linked to the Atlantic](#)  
303 [Multi-decadal Oscillation \(AMO\) of ocean-atmospheric circulations. The 11-year peak is well](#)  
304 [known solar signal while the 2-5 year periods apparently falls in ENSO frequency band.](#)~~cycles.~~  
305 These results ~~could be~~ better confirmed by applying the mathematical tools of SSA and  
306 wavelet ~~analyses.~~~~analysis.~~

307 **(Figure 2 & 3)**

308 To explore the stationary characteristics of these peaks obtained by the PCA, we have applied  
309 the Morlet based wavelet transform approach (Holschneider, 1995; Foufoula-Georgiou and  
310 Kumar, 1995; Torrence and Compo, 1998; Grinsted et. al., 2004). The wavelet spectrum  
311 identifies the main periodicities in the time series and helps to analyze the periodicities with  
312 respect to time. Figure 4 shows the wavelet spectrum for the a) Smoothed Sunspot number for  
313 solar activity (SSN) (b) Western Himalayan (WH) temperature variability record (c) Geomagnetic  
314 activity and (c) Troup Southern Oscillation Index (SOI). From the wavelet spectrum of sunspot  
315 time series (Figure 4a), the signal near 11-year is the strongest feature and is persistent during  
316 the entire series indicating the non-stationary behavior of the sunspot time series. The wavelet  
317 spectrum of SOI (figure 4c) shows strong amplitudes. However, due to non-stationary (time  
318 variant) character of the time series, the observed spectral peaks (power) split in the interval of  
319 2- 8 years. The wavelet power spectrum of the western Himalayan temperature variability  
320 (Figure 4b) reveals significant power concentration at inter-annual time scales of 3-5 years and  
321 at 11 years solar cycle. A dominant amplitude modes is also seen in the low frequency range at  
322 around 35-40 years (at periods 1930-1980) corresponding to AMO cycles. Our result agrees well  
323 with the results of other climate reconstructions (Mann et. al., 1995) from tree rings and other  
324 proxies. The observed variability in AMO periodicity has also been reported in other tree ring  
325 record (Gray et. al., 2004). The statistical significance of the wavelet power spectrum is tested  
326 by a Monte Carlo method (Torrence and Compo, 1998). The WH spectra depicting statistically  
327 significant powers [above the 95% significance level](#) at around 5 years, 11 years and 33 years

328 ~~above the 95% significance level,~~ suggests ~~possible a clear picture of the~~ imprint of sunspot-  
329 geomagnetic and ENSO phenomena on the tree ring data. ~~On shorter time scales, the~~ The  
330 wavelet power spectrum of the geomagnetic record (Fig. 4d) ~~also reveals statistically indicates~~  
331 significant power ~~at on shorter scales~~ around 2, 4-8, 11 years period.

332 **(Figure 4)**

333 In order to have better visualization of similar periods in two time series and for the  
334 interpretation of the results, cross wavelet spectrum has been applied. Figure 5 shows the cross  
335 wavelet spectrum of the a) SSN-WH temperature data b) WH data-SOI and c) SSN-SOI data. The  
336 contours (dark black lines) are the enclosing regions where wavelet cross power is significantly  
337 higher, at 95% confidence levels. The wavelet cross-spectra of WH-SSN (Fig.5a) show  
338 statistically significant high power over a period of 1895-1985 in 8-16 years band. It is seen that  
339 the WH-SOI cross-spectra (Fig. 5b), the high power is observed at 2-4 year band and 8-16 years  
340 as well. The SSN-SOI spectra (Fig. 5c) shows a strong correlation at 11 years solar cycle, which is  
341 stronger during 1910-1950 and 1960-2000 (Rigozo et. al., 2002, Rigozo et. al., 2003) suggesting  
342 the strongest El Nino and La Nina events indicating solar modulation on ENSO (Kodera, 2005;  
343 Kryjov and Park, 2007). These results show a good correspondence in response of growth of the  
344 tree ring time series during the intense solar activity. Hence the results strongly support the  
345 possible origin of these periodicities from Solar and ENSO events. The interesting conclusion  
346 from Fig. 5 is that WH-sunspot connections are strong at 11 years, ENSO-sunspot also exhibit  
347 strong power around 11 years; the WH-ENSO connections are spread over three bands, the 2-4  
348 y; 4-8 and 8-16 y, covering the solar cycle and its harmonics; the WH-geomagnetic exhibits  
349 strong connections around 2-4, 4-6, 11 years and 35-40 years indicating the influence of solar-  
350 geomagnetic activity on Indian temperature.

351 **(Figure 5)**

352  
353 The Singular spectral analysis (SSA) is performed for all the four data sets with window length of  
354 40. The SSA spectra with 40 singular values and its corresponding reconstructed series (varying  
355 from RC1-15 in some cases) are plotted are shown in Figure 6 &7. The important insights from  
356 SSA spectra are the identification of gaps in the eigen value spectra. As a rule, the pure noise

357 series produces a slowly decreasing sequence of singular values. The explicit plateau in the  
358 spectra represents the ordinal numbers of paired eigen triples. The eigen triples 2-3 for the  
359 sunspot data corresponds to 11 years period; eigen triples for 1-2,3-5,6-10,11-14 for the WH  
360 temperature data are related to harmonic with specific periods (periods 33-35y, 11y, 5y, 2y);  
361 eigen triples for 2-5,6-9,10-13 for the geomagnetic data are related to periods 11, 5, 2 years.  
362 The eigen triples for the SOI data represents to ~ 5-7, 2 years periods. In order to assess  
363 periodicities, the periodogram and the wavelet power spectra are plotted using the SSA  
364 reconstructed data (SSA-RC) (Figure 8). From the figure 8, the periodogram of SSA-RC of SSN  
365 and Geomagnetic data shows strong power at ~120, 10-11 years; the SOI data shows strong  
366 peaks at 6-9, 3 years & WH data shows strong power at ~32, ~10-11, 3-5 years. The wavelet  
367 spectra for all the SSA-RC data confirms the results excepts for the periods at ~120 years, which  
368 is beyond-as the maximum scaling period chosen for the present wavelet spectra is 64 years  
369 period. The coherency plot of the SSA-RC data sets (Figure 9) indicates a significant power at 33  
370 years, 11 years, 2-7 years in the WH temperature record suggesting the possible influences of  
371 Sunspot-geomagnetic activity and ENSO through tele-connection and hence significant role of  
372 these remote internal oscillations of the atmosphere-ocean system on the Indian climate  
373 system. Researchers have attributed these phenomena to internal ocean dynamics and involve  
374 ocean atmospheric coupling as well as variability in the strength of thermohaline circulations  
375 (Knight et. al., 2005; Delworth and Mann, 2000).

376 **(Figures 6, 7, 8 & 9)**

377 In general our result agrees well with earlier findings in the sense that statistically  
378 significant global cycles of coupled effects of Sunspot/geomagnetic and ENSO are present in the  
379 land based temperature variability record. However, there are certain striking features in the  
380 spectra that need to be emphasized regarding the western Himalayas temperature variability: i)  
381 Inter-annual cycles in period range of 3-8 years corresponding to ENSO in the wavelet spectra  
382 exhibit intermittent oscillatory characteristics throughout the large portion of the record (Fig 4);  
383 ii) The 11 years solar cycle in the cross wavelet spectrum of SSN and SOI (Figure 5) indicate the  
384 solar modulation in the ENSO phenomena (Kodera, 2005; Kryjov and Park, 2007). iii) The high  
385 amplitude at 11 years in the time intervals 1900-1995 with a strong intensity from 1900-1995

386 shows a good correspondence with the high temperature variability for the interval of high  
387 solar-geomagnetic activity. The Multi-decadal (30-40 years) periodicity identified here in  
388 Western Himalayan tree ring temperature record matches with North Atlantic sea surface  
389 temperature variability implying that the temperature variability in the western Himalayan is  
390 not a regional phenomenon, but a globally tele-connected climate phenomena associated with  
391 the global ocean-atmospheric dynamics system (Tiwari & srilakshmi, 2009; Delworth et. al.,  
392 1993; Stocker, 1994). The coupled ocean-atmosphere system appears to transport energy from  
393 the hot equatorial regions towards Himalayan territory in a cyclic manner. These results may  
394 provide constraints for modeling of climatic variability over the Indian region and ENSO  
395 phenomena associated with the redistribution of temperature variability. The solar-  
396 geomagnetic effects play a major role in abnormal heating of the land surface thereby indirectly  
397 affects the atmospheric temperature gradient between the land-ocean coupled systems. In the  
398 present work, the connections between solar/geomagnetic activity and ENSO on the WH time  
399 series are found to be statistically significant, especially when they are studied over contrasting  
400 epochs of respectively high and low solar activity. The correlation plots for the SSA-RC data sets  
401 of WH-sunspot, WH-aa index, WH-SOI and Sunspot-aa index are plotted in figure 10. It is  
402 noticed that there is a correlation plots for the Geomagnetic-sunspot activity has a maximum  
403 correlation value at 1 year lag suggesting the strong influence of sunspot & geomagnetic forcing  
404 on one another. The cross-correlation plot for the WH data and the SOI represents a maximum  
405 value at zero lag. The correlations plot for WH-sunspot & WH-geomagnetic index exhibits  
406 almost the identical results suggesting the possible impact of solar activities on the Indian  
407 temperature variability.

408 **(Figures 10)**

409 The net effect of solar activity on temperature record therefore appears to be the result  
410 of cooperating or counteracting influences of earth's magnetic activity on the shorter and  
411 longer periods, depending on the indices used; scale-interactions, therefore, appear to be  
412 important. Nevertheless, the link between Indian climate and solar/geomagnetic activity  
413 emerges as having the strong evidence; next is the ENSO-solar activity connection.

414

415 **5. Conclusions:**

416 In the present paper, we have studied and identified the periodic patterns from the published  
417 Indian temperature variability records using the modern spectral methods of Singular spectral  
418 analysis (SSA)-Wavelet methods. The application of wavelet analysis for the SSA reconstructed  
419 time series, along with the removal of noise in the data identifies the existence of a high-  
420 amplitude, recurrent, multi-decadal scale patterns that are present in Indian temperature  
421 records. The power spectra of WH temperature data shows strong high power at ~62 years, 32-  
422 35 years, 11 years, 5 years and 2-3 years suggesting a strong influence of solar-geomagnetic-  
423 ENSO effects on the Indian climate system. The presence of dominant amplitude at 33-year  
424 cycle periodicity corresponds to Atlantic Multidecadal Oscillation (AMO) cycles. It also suggests  
425 the Sun-temperature variability probably involving the induced changes in the basic state of the  
426 atmosphere. The 30-40 yrs periodicity in Western Himalayan tree ring temperature record  
427 matches with the global signal of the coupled ocean-atmospheric oscillation (Delworth et. al.,  
428 1993; Stocker, 1994) implying that the temperature variability in Himalayan is not a regional  
429 phenomenon, but seems to be tele-connected phenomena with the global ocean-atmospheric  
430 climate system. The coherency plots of the SSA reconstructed WH-Sunspot; WH-geomagnetic  
431 and WH-SOI data sets show strong spectral signatures in the whole record confirming the  
432 possible influences of Sunspot-geomagnetic activities and ENSO through teleconnection and  
433 hence the significant role of these remote internal oscillations of the atmosphere-ocean system  
434 on the Indian temperatures. We conclude that the signature of solar-geomagnetic activity  
435 affects the surface air temperatures of Indian subcontinent. However, long data sets from the  
436 different sites on the Indian continent are necessary to identify the influences of the 120 years  
437 solar-geomagnetic cycles.

438

439 **Acknowledgements**

440 | The authors are extremely thankful to [the Editor Dr. Stéphane Vannitsem and](#) the anonymous  
441 reviewers for their professional comments, meticulous reading of the manuscript and valuable  
442 suggestions to improve the manuscript. The authors thank Dr. Ram Ratan Yadav, Birbal Sahni  
443 Institute of Palaeobotany, India for providing the Western Himalayan data. The authors



444 acknowledge Dr. Francisco Javier Alonso of University of Extremadura for using the SSA routine  
445 in a MATLAB environment. We are thankful to Dr. Grinsted and his colleagues for providing the  
446 wavelet software package. First author acknowledged the Head, University Centre for Earth &  
447 Space Sciences, University of Hyderabad for providing the facilities to carry out this work. RKT is  
448 grateful to DAE for RRF.

449

#### 450 **References**

- 451 Alonso, F. J., Castillo, J., and Pintado, P. (2005), "Application of Singular Spectrum Analysis to the  
452 Smoothing of Raw Kinematic Signals," *Journal of Biomechanics*, 38(5), 1085–1092.
- 453 Appenzeller, C., Stocker, T. F., and Anklin, M. (1998). North Atlantic Oscillation Dynamics Record in  
454 Greenland Ice Cores. *Science*, 282(5388), 446–449.
- 455 Barnett, T.P., et al. (1989). The effect of Eurasian snow cover on regional and global climate  
456 variations. *J. Atmos. Sci.*, 48, 661–685.
- 457 Benestaed, R.E., and Schmidt, G.A., (2009), Solar trends and global warming, *Journal of Geophysical*  
458 *research*, P 114.
- 459 Bhattacharyya A, LaMarche VC, and Telewski FW, (1988) Dendrochronological reconnaissance of the  
460 conifers of Northwest India, *Tree-Ring Bull.*, 48: 21-30.
- 461 Bhattacharyya A, and Chaudhary V, (2003) Late-summer temperature reconstruction of the Eastern  
462 Himalayan Region based on tree-ring data of *Abies densa*, *Arct. Antarct. Alp. Res.*, 35(2): 196-202.
- 463 Bhattacharyya A, and Yadav RR, (1996) Dendrochronological reconnaissance of *Pinus wallichiana* to  
464 study glacial behaviour in the western Himalaya. *Current Science*, 70 (8): 739-744.
- 465 Bhattacharyya A, Shah, Santosh K, and Chaudhary V, (2006) Would tree-ring data of *Betula utilis* be  
466 potential for the analysis of Himalayan Glacial fluctuations?, *Current Science*, 91(6): 754-761.
- 467 Bhattacharyya A, Yadav RR, Borgaonkar HP, & Pant GB, (1992) Growth ring analysis of Indian tropical  
468 trees: Dendroclimatic potential, *Current Science*, 62: 736-741.
- 469 Bhattacharyya, A. and Yadav, R.R., (1992) Tree growth and recent climatic changes in the western  
470 Himalaya, *Geophytology*, 22, 255-260.
- 471 Bigg GR, (1996) *The oceans and Climate*, Cambridge University Press, Cambridge, 1-266.

472 Borgeonkar HP, Pant GB, & Rupa Kumar k, (1996) Ring width variations in Cedrus deodara and its  
473 climatic response over the Western Himalaya. Intern. J. Climatol. 16: 1409-1422.

474 Broomhead, D.S., and King, G.P., (1986). Extracting qualitative dynamics from experimental data,  
475 Physica D 20, 217–236.

476 Budyko, M. I. (1969). The effect of solar radiation variations on the climate of the Earth. Tellus, 21,  
477 611–619

478 Cane MA, (1992) Tropical Pacific ENSO models: ENSO as a mode of the coupled system. In: Climate  
479 System Modelling, Ed: K.E. Trenberth, Cambridge University Press, Cambridge, 583-614.

480 Chaudhary V, Bhattacharyya A, and Yadav RR, (1999) Tree-ring studies in the Eastern Himalayan  
481 region: Prospects and problems, IAWA, .20(3): 317-324.

482 Chowdary, J. S., John, N., and Gnanseelan, C. (2014). Interannual variability of surface air-  
483 temperature over India: impact of ENSO and Indian Ocean Sea surface temperature. Int. J.  
484 Climatol., 34, 416–429.

485 Chowdary, J.S., Gnanseelan, C., Vaid, B.H., and Salvekar, P.S. (2006). Changing trends in the tropical  
486 Indian Ocean SST during La Nina years. Geophys. Res. Lett., 33, L18610. doi:10.1029/  
487 2006GL026707.

488 Cole JE, Fairbanks RG, and Shen GT, (1993) Recent variability in the Southern Oscillation: Isotopic  
489 results from a Tarawa Atoll coral. Science, 260: 1790-1793.

490 De Freitas, C., and Mclean, J. (2013). Update of the Chronology of Natural Signals in the Near Surface  
491 Mean Global Temperature Record and the Southern Oscillation Index. International Journal of  
492 Geosciences, 4 (1), 234–239.

493 Delworth T, and Mann M, (2000) Observed and Stimulated multidecadl variability in the Northern  
494 Hemisphere, 16: 661-676.

495 Delworth T, Manabe S & Stouffer RJ (1993) Interdecadal variations of the thermohaline circulation in  
496 a coupled ocean-atmosphere model. J. Climate 6: 1991-2011.

497 El-Borie, M.A., Shafik, E., Abdel-Halim, A.A., El-Monier, S., (2010), Spectral analysis of solar  
498 variability and their possible role on the global warming (1880-2008), Journal of Enviromental  
499 Protection, 1, pp 111-120.

500 El-Borie, M.A., Al. Thoyaib, S.S, Al-Sayed, N., (2007), The 2nd Inter. CPMS, 302.

501 El-Borie, M.A., and Al-Thoyaib, S.S., (2006), Can we use the aa geomagnetic activity index to predict  
502 partially the variability in global mean temperature, *Journal of Physical Sci.*,1(2), pp 67–74.

503 Feng, S.H., Kaufman, D., Yoneji, S., Nelson, D., Shemesh, A., Huang, Y., Tian, J., Bond, G., Benjamin, C.,  
504 and Brown, T. (2003). Cyclic Variation and Solar Forcing of Holocene Climate in the Alaskan  
505 Subarctic. *Science*, 301, 1890–1893.

506 Foufoula-Georgiou E, and Kumar P, (Eds.), (1995) *Wavelets in Geophysics*, Academic San Diego, Calif.,  
507 373pp.

508 Friis, C.E., and Lassen, K. (1991). Length of the Solar Cycle: An Indicator of Solar Activity Closely  
509 Associated with Climate. *Science*, 254 (5032), 698–700.

510 Friis, C.E., and Svensmark, H. (1997). What do we really know about the sun- climate connection?,  
511 *Adv. Space Res.*, 20, 415, 913–9211.

512 Frohlich, C., and Lean, J. (2004). Solar radiative output and its Variability: Evidence and Mechanisms.  
513 *The Astron Astropys Rev.*, 12, 273–320.

514 Golyandina, N., Nekrutkin, V. V., and Zhigljavski, A. A. (2001), *Analysis of Time Series Structure:*  
515 *SSA and Related Techniques*, Boca Raton: CRC Press.

516 Gray L.J., Beer, J., Geller, M., Haigh, J.D., Lockwood, M., Matthes, K., Cubasch, U., Fleitmann, D.,  
517 Harrison, G., Hood, L., Luterbacher, J., Meehl, G.A., Shindell, D., van Geel B., and White, W., (2010).  
518 Solar influences on climate, *Reviews of Geophysics*, 48, RG 4001, doi: 10.1029/2009RG000282.

519 Gray ST, Graumlich LJ, Betancourt JL, and Pederson GT, (2004) A tree-ring based reconstruction of the  
520 Atlantic Multidecadal Oscillation since 1567 A.D, *Geophys. Res. Lett.* , 31: L12205,  
521 doi:10.1029/2004GL019932.

522 Gray, W. M., Sheaffer, J. D., and Knaff, J. A. (1992). Hypothesized mechanism for stratospheric QBO  
523 influence on ENSO variability. *Geophys. Res. Lett.*, 19, 107–110.

524 Grinsted A, Moore JC, Jevrejeva S (2004) Application of the cross wavelet transform and wavelet  
525 coherence to geophysical time series, *Nonlin. Processes Geophys.*, 11: 561–566,  
526 doi:10.5194/npg-11-561-2004

527 Gu, D., and Philander, S.G.H., (1995). Secular changes of annual and inter-annual variability in the  
528 tropics during the past century, *J. Clim.* 8, 64–876.

529 Holschneider M (1995) *Wavelets: An Analysis Tool*, Oxford University Press, New York, 455.

530 Horel, J.D., and Wallace, J.M.(1981). Planetary-scale atmospheric Phenomena associated with the  
531 Southern Oscillation, *Monthly weather review*, 109, 813-829.

532 Hughes MK (1992) Dendroclimatic evidence from the Western Himalaya. In: R.S. Bradley &  
533 D.Jones(eds.),*ClimatesinceAD 1500:4* 15-431.Routledge.London.

534 Jevrejeva S, Moore JC, Grinsted A (2003) Influence of the Arctic Oscillation and El Niño-Southern  
535 Oscillation (ENSO) on ice conditions in the Baltic Sea: The wavelet approach, *J. Geophys. Res.*,  
536 108(D21), 4677, doi:10.1029/2003JD003417.

537 Ji JF, Shen J, Balsam W, Chen J, Liu L & Liu XQ, (2005) Asian monsoon oscillations in the northeastern  
538 Qinghai-Tibet Plateau since the late glacial as interpreted from visible reflectance of Qinghai Lake  
539 sediments, *Earth and Planetary Science letters* 233: 61-70.

540 Kasatkina, E.A., Shumilov, O.I., and Krapiec, M.(2007). On periodicities in long term climatic variations  
541 near 68°N, 30°E. *Adv. Geosci*, 13, 25–29.

542 Kiladis, G.N., and Diaz, F.H. (1989). Global Climatic Anomalies Associated with Extremes in the  
543 Southern Oscillation. *J. Climate*, 2, 1069–1090.

544 Knight JR, Allan RJ, Folland CK, Vellinga M, and Mann ME, (2005) A signature of persistent natural  
545 thermohaline circulation cycles in observed climate'. *Geophys. Res. Lett.*, 32, L20708,  
546 doi:10.1029/2005GL024233.

547 Kodera, K., and Y.Kuroda (2005). A possible mechanism of the spatial structure of the North Atlantic  
548 Oscillation, *Journal of Geophysical Research*, 110, D02111, doi: 10.1029/2004JD005258.

549 Kothwale, D.R., Munot, A.A., and Krishna Kumar, K. (2010). Surface air temperature variability over  
550 India during 1901-2007 and its association with ENSO. *Climate Research*, 42, 89–104,  
551 doi:10.3354/cr00857.

552 Kryjov, V.N., and Park, Chung-Kyu, (2007). Solar modulation of the El-Nino/Southern Oscillation  
553 impact on the Northern Hemisphere annular mode, *Geophysical research letters*, Vol. 34,  
554 L10701, doi: 10.1029/2006GL028015.

555 Lean, J.L. and Rind, D.H., (2008), How natural and anthropogenic influences alter global and  
556 regional surface temperatures: 1889 to 2006, *Journal of Geophysical Research, Letter*, p 35.

557 Lean, J., Beer, J., and Bradley, R. (1995). Reconstruction of solar irradiance since 1610: Implications  
558 for climate change. *Geophys. Res.Lett.*, 22, 3195-3198.

559 Mann ME, Park J, and Bradley RS, (1995) Global interdecadal and century-scale climate oscillations  
560 during the past 5 centuries, *Nature*, 378: 266–27.

561 Meehl, G.A., Arblaster, J.M., Matthes, K., Sassi, F., and Van Loon, H. (2009). Amplifying the Pacific  
562 climate system response to a small 11-year solar cycle forcing. *Science*, 325, 1114–1118.

563 Mendoza B, Perez-Enriquez R, and Alvarez-Madrigo M, (1991) Analysis of solar activity conditions  
564 during periods of El Nino events, *Ann. Geophysicae*, 9: 50-54.

565 [Minobe, S. \(1997\). A 50-70 year climatic oscillation over the North Pacific and North](#)  
566 [America. \*Geophysical Research Letters\*, 24\(6\), 683-686.](#)

567 Mokhov, I. I., Eliseev, A.V., Handorf, D., Petukhov, V.K., Dethloff, K., Weishiemeier, A., and  
568 Khvorostyanov, D. V. (2000). North Atlantic Oscillation: Diagnosis and simulation of decadal  
569 variability and its long period evolution. *Atmospheric and Ocean physics*, 36, 555–565.

570 Nicolson, S. E. (1997). An analysis of the Enso signal in the tropical Atlantic and western Indian  
571 oceans. *Int. J. Climatol.*, 17, 345–375.

572 [Ogurtsov, M. G., Nagovitsyn, Y. A., Kocharov, G. E., & Jungner, H. \(2002\). Long-period cycles of](#)  
573 [the Sun's activity recorded in direct solar data and proxies. \*Solar Physics\*, 211\(1-2\), 371-](#)  
574 [394.](#)

575 Pant, G.B., and Rupa Kumar, K. (1997). *Climates of South Asia*. John Wiley and Sons, Chichester, 320  
576 pp.

577 Philander SG, (1990) El Nino, La Nina and the Southern Oscillation. Academic Press, London, 1-293.

578 Proctor, C.J., Baker, A., and Barnes, W. L. (2002). A three thousand year record of North Atlantic  
579 Climate. *Clim.Dyn*, 19, 449–454.

580 Reid GC and Gage KS, (1988) The climatic impact of secular variations in solar irradiance, in *Secular*  
581 *Solar and geomagnetic Variations in the Last 10000 years'*, Eds. F.R. and A.W. Wpplendale, NATO  
582 AS Series, Kluwer, Dordrecht, 225-243.

583 Reid GC, (1991) Solar irradiance variations and global Ocean Temperature, *Journal of Geomagn.*  
584 *Geoelectr.*, 43: 795-801.

585 Rigozo NR, Noredmann DJR, Echer E, Zanandrea A, Gonzalez WD, (2002) Solar variability effects  
586 studied by tree-ring data wavelet analysis, *Adv. Space Res.*, 29(12): 1985-1988.

587 Rigozo NR, Vieira Lea, Echer E, Nordemann DJR, (2003) Wavelet analysis of Solar-ENSO imprints in  
588 tree-ring data from Southern Brazil in the last century, *Climatic change*, 60: 329-340.

589 Rigozo, N. R., Nordeman, D. J. R., Echer, E., Vieira, L. E. A., Echer M. P. S. and Presets, A.(2005). Tree-  
590 ring width wavelet and spectral analysis of solar variability and climatic effects on a Chilean  
591 cypress during the last two and a half millennia. *Climate of the Past Discussions*, 1, 121–135.

592 Rigozo, N. R., Nordeman, D.J.R., Silva, H.E., Echer, M.P.S. and Echer, E. (2007). Solar and climate signal  
593 records in tree ring width from Chile (AD1587–1994). *Planetary and Space Science*, 55, 158–164.

594 Shah Santosh K, Bhattacharyya A, and Chaudhary V, (2007) Reconstruction of June-September  
595 Precipitation based on tree-ring data of Teak (*Tectona grandis* L.) from Hoshangabad, Madhya  
596 Pradesh, India. *Dendrochronologia*, 25: 57-64.

597 [Schlesinger, M E and Ramankutti, N, 1994. An oscillation in the global climate system of period 65-70](#)  
598 [years. \*Nature\* , vol 367, pp723-726](#)

599 Steinhilber, F., Beer, J. and Frohlich, C. (2009). Total solar irradiance during the Holocene. *Geophys.*  
600 *Res. Lett.*, 36, L19704.

601 Stocker TF (1994). The variable ocean. *Nature* 367: 221-222.

602 Tiwari RK, and Srilakshmi S, (2009). Periodicities and non-stationary modes in tree ring temperature  
603 variability record of the Western Himalayas by multitaper and wavelet spectral analyses, *Current*  
604 *Science*, 97, 5: 705-709.

605 [Tiwari \(2005\) . \*Geospectroscopy\*, Capital Publ Co, New Delhi. Page 308.](#)

606 Torrence C, Compo GP, (1998). A practical guide to wavelet analysis, *Bull. Am. Meteorol. Soc.*, 79: 61–  
607 78

608 Torrence C, Webster P, (1999). Interdecadal changes in the ENSO-Monsoon System, *J.Clim.*, 12:  
609 2679–2690.

610 Trenberth K, and Hoar TJ, (1997). El Nino and climate change. *Geophys. Res. Lett.*, 24: 3057–3060.

611 Tsonis, A. A., Elsner, J. B., Hunt, A. G., and Jagger, T. H. (2005). Unfolding the relation between global  
612 temperature and ENSO. *Geophys. Res. Lett.*, 32, L09701.

613 Vautard, R., and Ghil, M. (1989). Singular spectrum analysis in nonlinear dynamics, with applications  
614 to paleoclimatic time series. *Phys. D*, 35, 395–424.

615 Weng, H., and K.-M. Lau, 1994: Wavelets, period doubling, and time-frequency localization with  
616 application to organization of convection over the tropical western Pacific. *J. Atmos. Sci.*, 51,  
617 2523–2541.

618 Wiles, G. C., D'Arrigo, R. D., and Jacoby, G. C. (1998). Gulf of Alaska atmosphere-ocean variability over  
619 recent centuries inferred from coastal tree-ring records, *Climatic Change*, 38,

620 Yadav RR, Park WK, and Bhattacharyya A, (1999) Spring-temperature variations in western Himalaya,  
621 India, as reconstructed from tree-rings: AD 1390-1987, *The Holocene*, 9(1): 85-90.

622 Yadav RR, Park WK, Singh J & Dubey B, (2004) Do the western Himalayas defy global warming?,  
623 *Geophysical Research Letters* 31: L17201, doi: 10.1029/2004GL020201.

624 Yasunari, T. (1985). Zonally propagating modes of the global east–west circulation associated with  
625 the Southern Oscillation. *J. Meteorol. Soc. J.*, 63, 1013–1029.

626

627

628

629

630

631

632

633

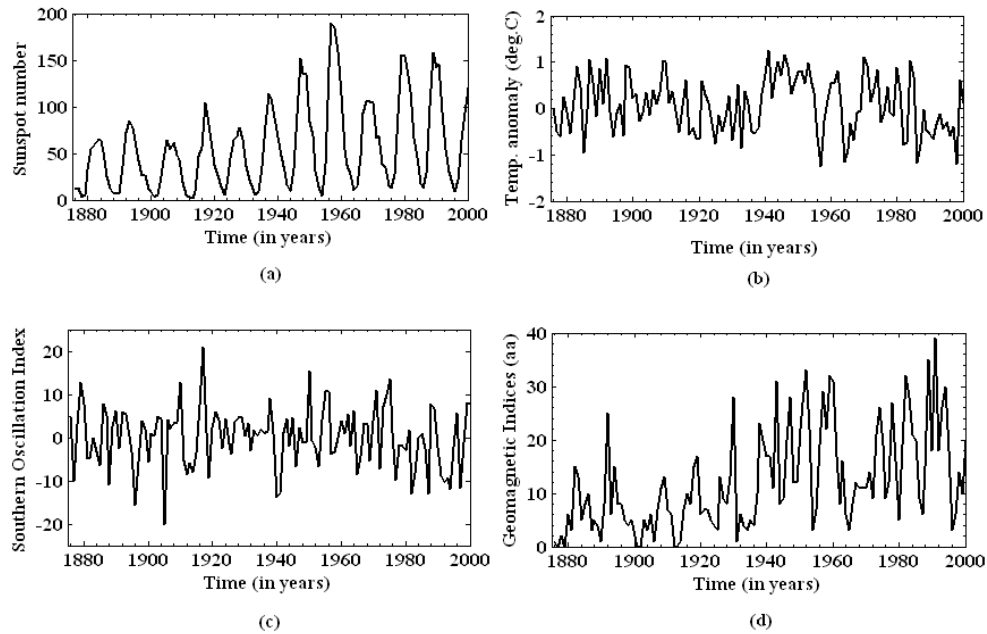
634

635

636

637

638

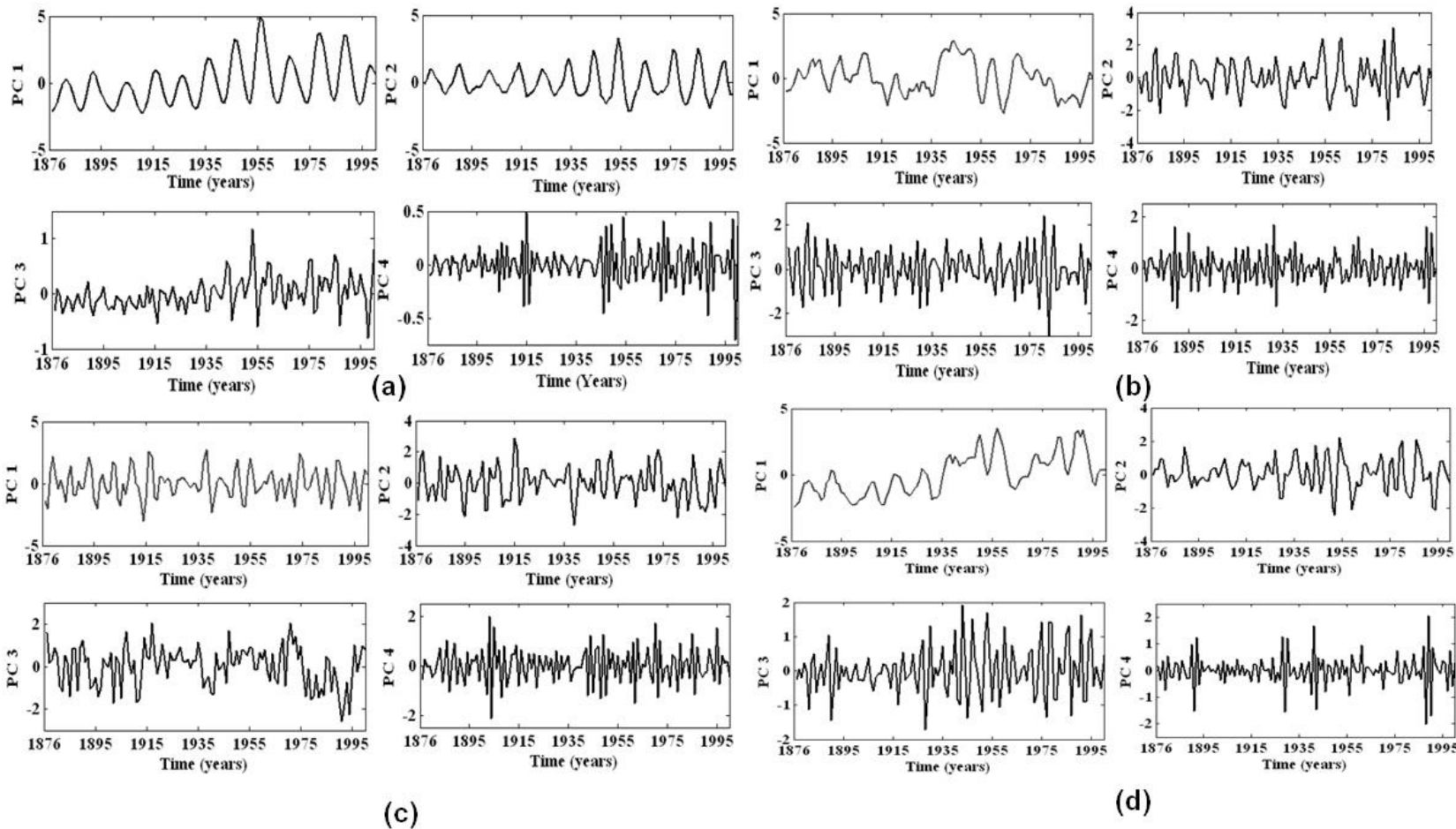


639  
 640 **Figure 1. Time series data of (a) Sunspot Index (b) the mean pre-monsoon temperature**  
 641 **anomalies of the Western Himalayas (Yadav et. al., 2004) (c) Southern Oscillation Index**  
 642 **(SOI) and (d) Geomagnetic Indices (aa indices) for common period 1876-2000.**

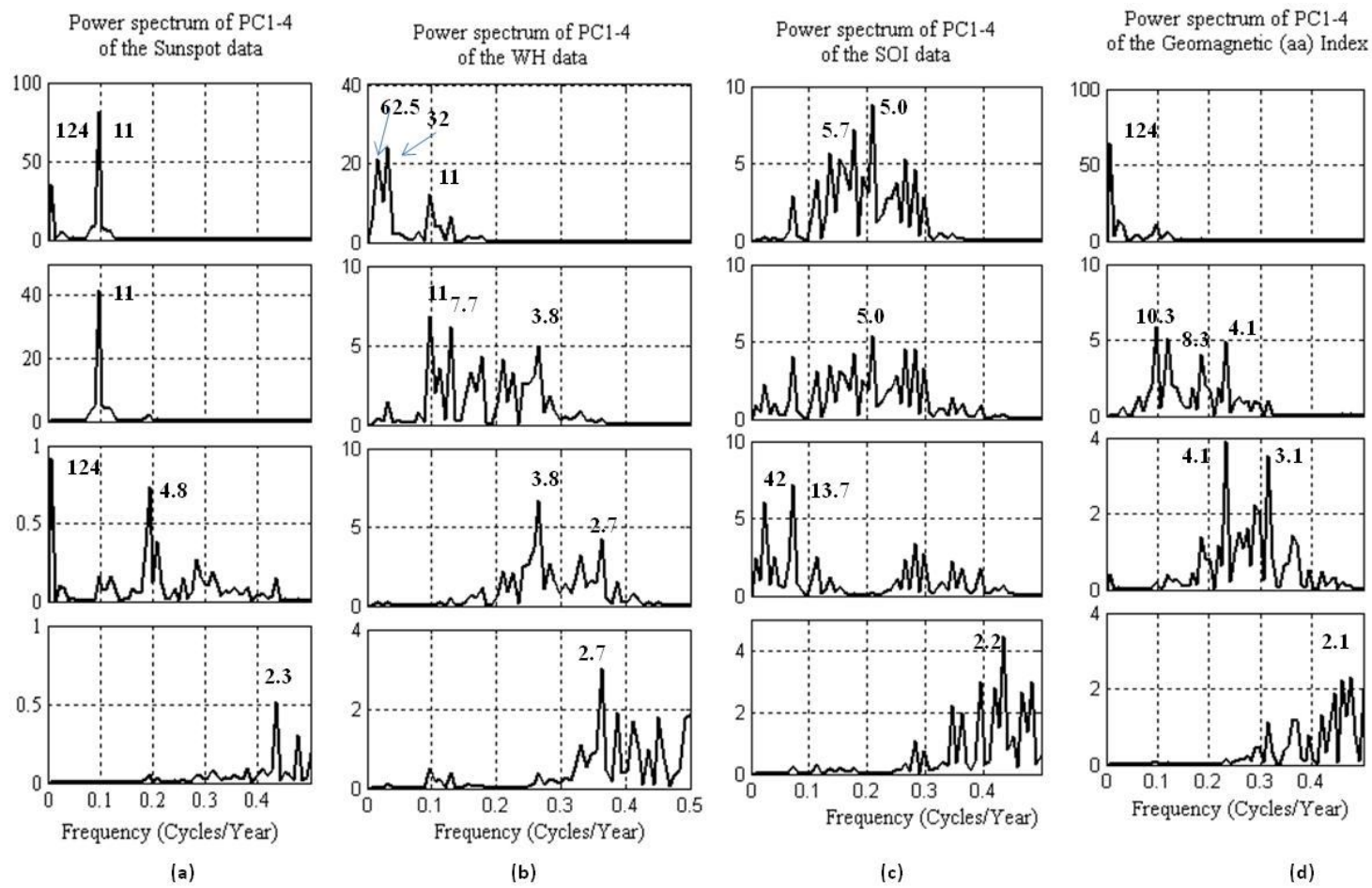
643

644



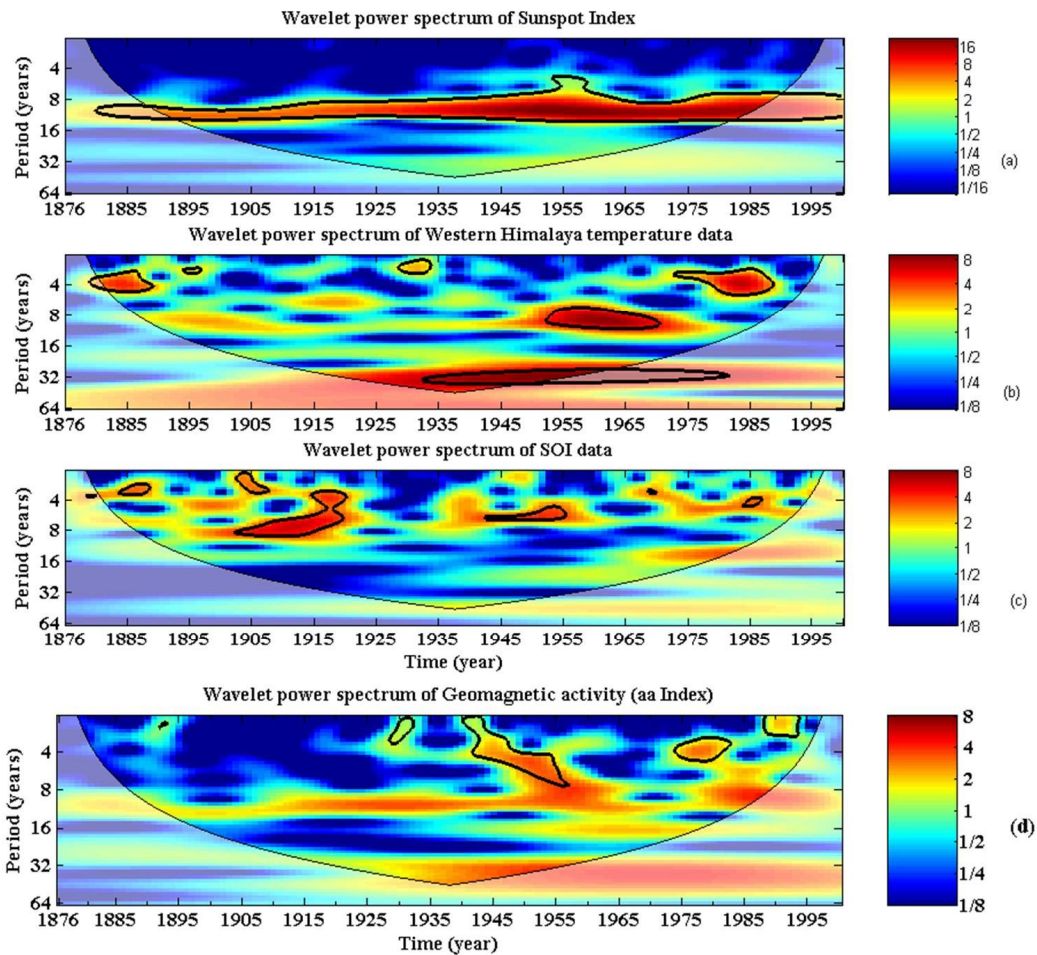


645  
 646 **Figure 2. First four principal components (PCs:1-4) for time series (a) Sunspot numbers (b) the mean pre-monsoon temperature anomalies**  
 647 **of the Western Himalayas (c) SOI index and (d) Geomagnetic Indices (aa indices) for the period 1876-2000.**



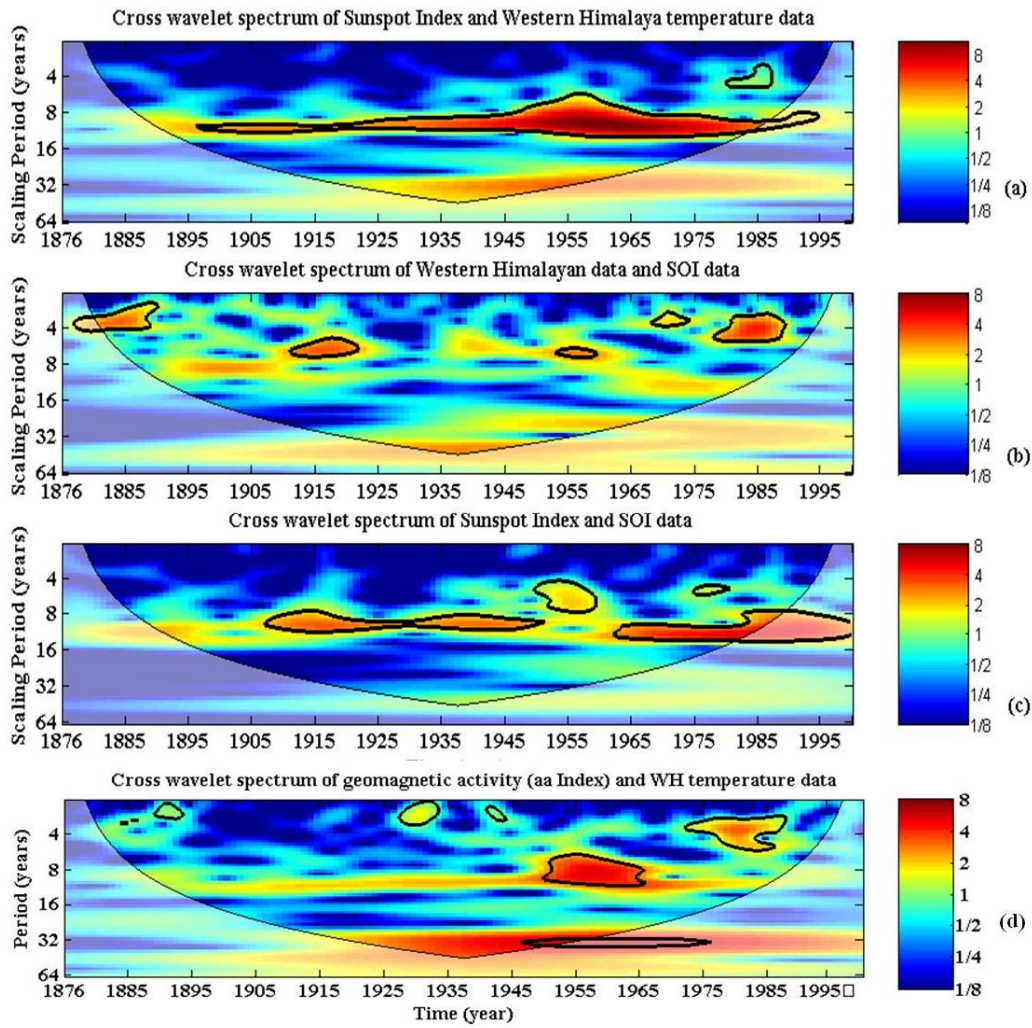
648

649 **Figure 3. Power spectra of the first four principal component (PCs) (PC1-4 shown in Fig. 2) for all the data sets with their significant**  
 650 **periodicities at 124, 11, 4 and 2.8 years are indicated in bold letters.**



651  
 652 **Figure 4. Wavelet power spectrum of (a) Sunspot Number (b) Western Himalaya temperature**  
 653 **data (c) Southern Oscillation Index (SOI) and (d) Geomagnetic activity (aa Indices) with cone**  
 654 **of influence (lighter shade smooth curve) and black lines indicate significant power on 95%**  
 655 **level compared to red noise based on first order auto-regressive (AR(1)) coefficient. The**  
 656 **legend on right indicates the cross-wavelet power.**

657



659

660

661

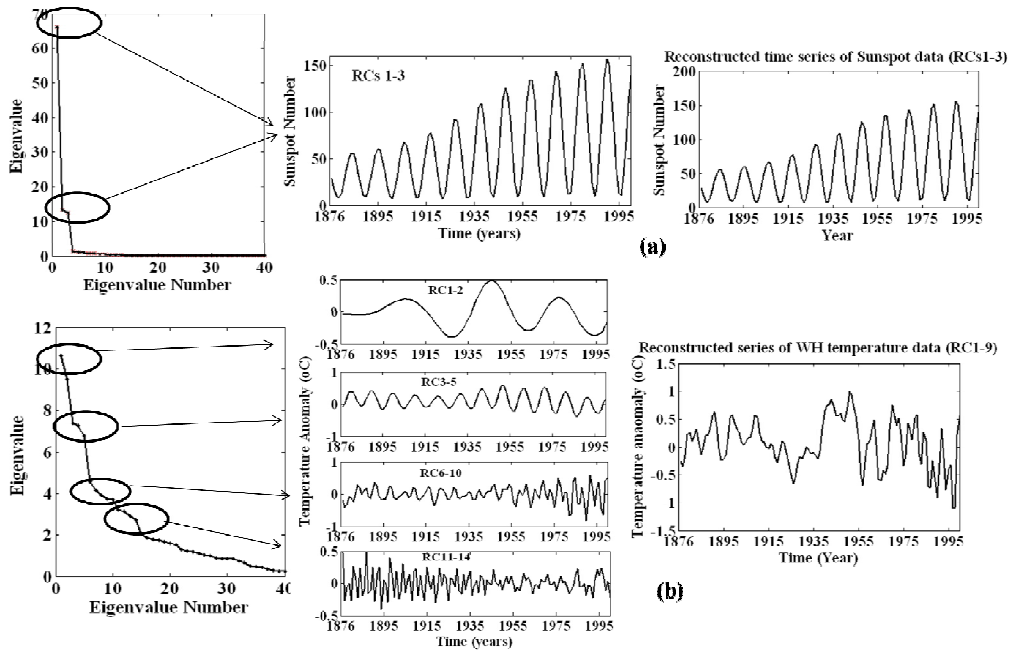
662

663

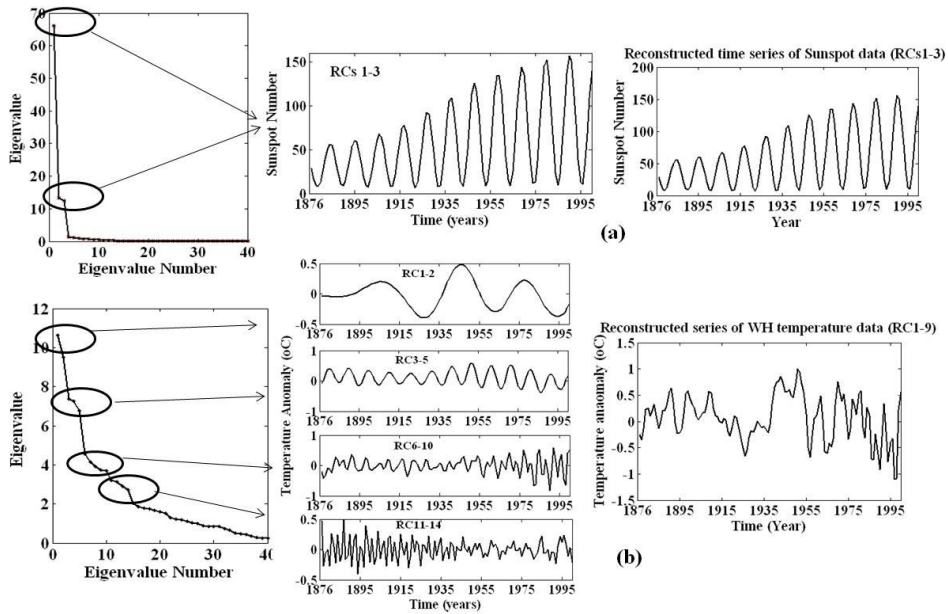
**Figure 5. Cross Wavelet spectrum between (a) Sunspot number-Western Himalayan data (b) Western Himalayan-Southern Oscillation Index (c) Sunspot number- Southern Oscillation Index and (d) Geomagnetic: aa indices-Western Himalayan data with cone of influence (lighter shade smooth curve) and black lines indicate significant power on 95%**



664 level compared to red noise based on AR(1) coefficient. The legend on right indicates the  
 665 cross-wavelet power.

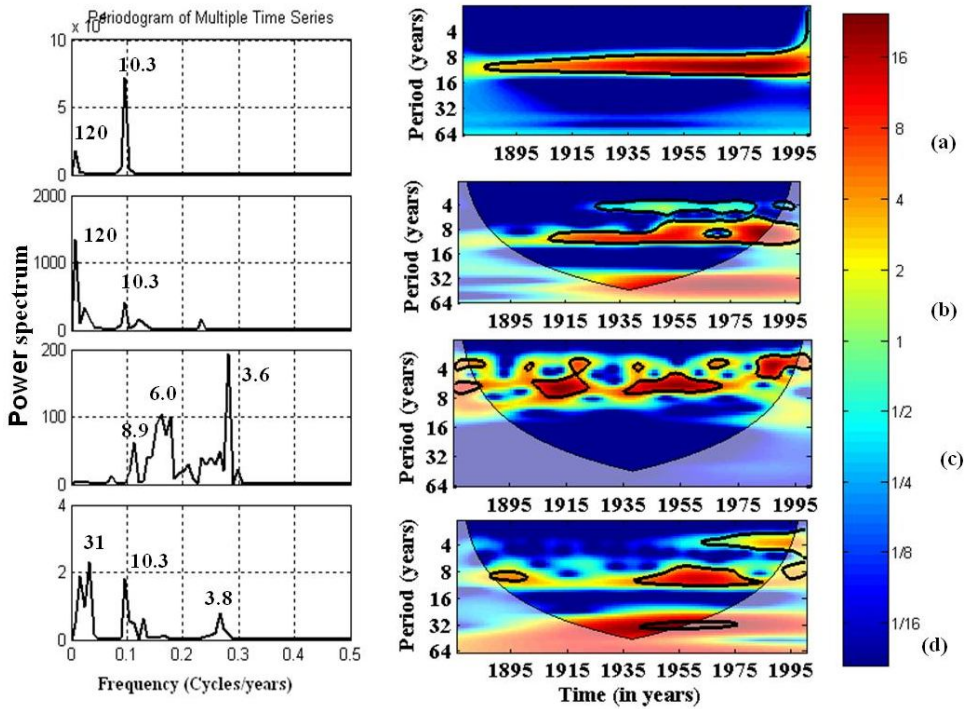


666  
 667 **Figure 6. Singular spectra with its SSA decomposed components & its reconstructed time series for (a) Sunspot Number and (b) Western Himalaya temperature data.**  
 668  
 669



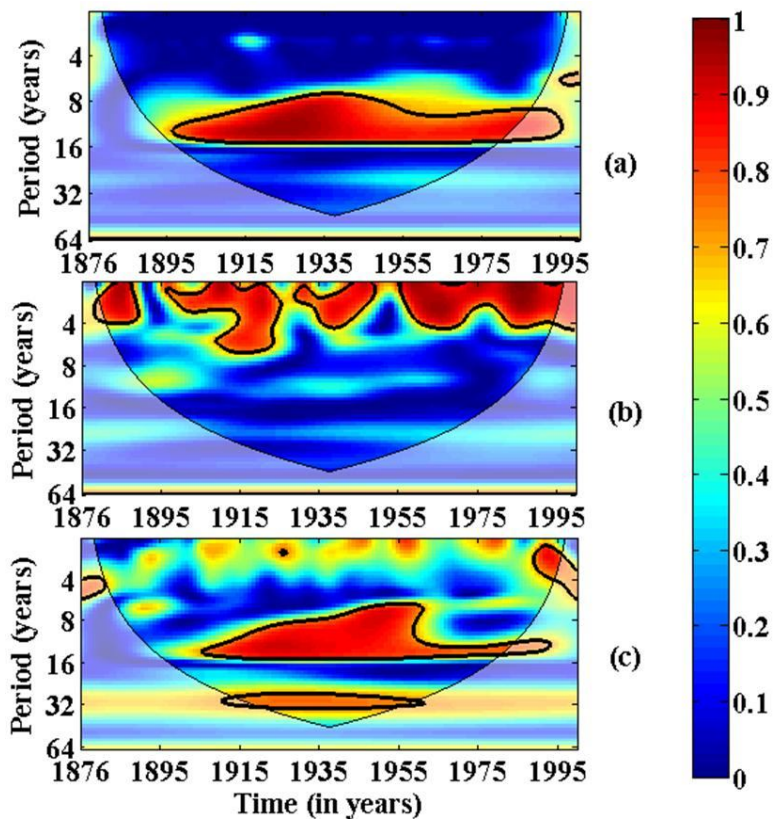
670

671 **Figure 7. Singular spectra with its SSA decomposed components & its reconstructed time**  
 672 **series for (c) SOI and (d) Geomagnetic activity (aa Indices).**



673  
 674 **Figure 8. Power spectrum and Wavelet power spectrum of SSA reconstructed (a) Sunspot**  
 675 **data (b) Geomagnetic Indices (aa index) (c) SOI index and (d) the Western Himalayas**  
 676 **temperature data with cone of influence (lighter shade smooth curve) and black lines indicate**  
 677 **significant power on 95% level compared to red noise based on AR(1) coefficient. The legend**  
 678 **on right indicates the cross-wavelet power.**

679  
 680  
 681  
 682  
 683



684

685 **Figure 9.** Squared wavelet coherence plotted for the SSA reconstructed time series between  
 686 (a) WH-SSN (b) WH-SOI and (c) WH-aa index with cone of influence (lighter shade smooth  
 687 curve) and black lines indicate significant power on 95% level compared to red noise based on  
 688 AR(1) coefficient.

689

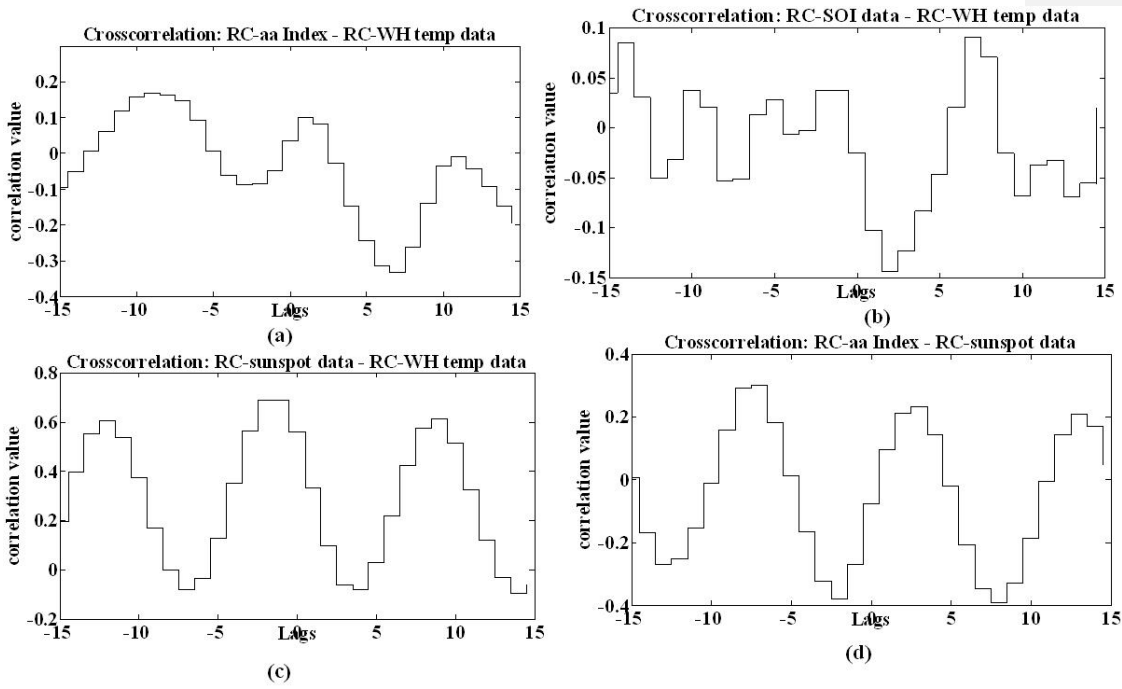
690

691

692



693



694

695 **Figure 10. Cross-correlation of SSA reconstructed time series of (a) aa Index-Western**  
696 **Himalayan (WH) temperature data; (b) SOI-WH temperature data; (c) sunspot –WH data and**  
697 **(d) aa Index-sunspot data.**

698

699

700

701

702

703

704 **Reply to the Editor comments on "Wavelet analysis of the singular spectral reconstructed**  
705 **time series to study the imprints of solar-ENSO-Geomagnetic activity on Indian climate' by S.**  
706 **Sri Lakshmi and R.K.Tiwari**

707

708 The authors are very much thankful to the Editor for his professional comments and  
709 suggestions for improving the manuscript. We have incorporated the Editor's suggestions  
710 accordingly:

711

712 **Line 61: ENSO is not "producing" droughts. I suggest to replace 'produces' by 'is associated**  
713 **with... in different part of the world'.**

714 As suggested by the Editor, we have modified the sentence in the Line 61.

715

716 **Lines 89-90. I do not understand the sentence. Temperature is subject to climate change.**

717 **Please rephrase.**

718 As suggested we have modified the text accordingly in the Line 89-90.

719

720 **Line 98: Shah et al. What is the corresponding year?**

721 The year corresponding to Shah et. al. 2007, has been added in Line 98.

722

723 **Line 127: Maybe better to remove "potentially"**

724 The word "potentially" has been removed.

725

726 **Line 138: put 'in total' after 'trees'.**

727 The line 138 has been modified.

728

729 **Lines 151-153. The sentence is not clear at all. Please rephrase. I would suggest something**  
730 **like: ..., and are uncorrelated. The different PCs capture part of the variance and are ranked**  
731 **depending on their corresponding percentage variance.**

732

733 The line 151-153 has been rephrased accordingly.

734

735 **Lines 303, 328, 360, you mentioned the peaks in the spectra, in particular the 62 and 32-35**

736 **year periods. It is not enterily clear to what you are associated these peaks... harmonics of**

737 **signals (and in this case clarify)? AMO? Sometimes you mentioned that all of them are**

738 **associated with solar-geomagnetic forcings, sometimes not. It should be clarified.**

739

740 The text in the lines as indicated above are modified for better clarification.

741

742 With kind regards

743 Srilakshmi

744